An ADP Framework for Flexibility and Cost Aggregation: Guarantees and Open Problems

Maísa Beraldo Bandeira, Timm Faulwasser, Alexander Engelmann
Institute of Energy Systems, Energy Efficiency and Energy Economics (ie3)
TU Dortmund University, Dortmund, Germany
maisa.bandeira@tu-dortmund.de, {timm.faulwasser, alexander.engelmann}@ieee.org

***Abstract*—With the increasing amount of Distributed Energy Resources (DERs), coordination of Distribution Grid Operators (DSOs) and Transmission Grid Operators (TSOs) is of paramount importance. Managing a large number of DERs at the TSO level is, however, challenging. To address this problem, flexibility aggregation is a topic of frequent research activities. Aggregation means to describe the *combined* flexibility of the DERs at the vertical grid coupling between DSO and TSO. Existing works are often limited with respect to guaranteeing feasibility, with respect to efficient numerical implementation, and in terms of quantification of the cost of DER usage. In the present paper, we investigate aggregation based on Approximate Dynamic Programming (ADP). We propose efficient numerical aggregation schemes using tools from computational geometry thus avoiding the need to solve multiple OPF problems. We rely on different variants of the `DistFlow` model for radial grids, which are computationally efficient. This allows to model of current and voltage limits and enables the consideration of voltage dependencies in the aggregation. Furthermore, we propose a method for cost aggregation and identify open problems of flexibility aggregation.**

***Index Terms*—Flexibility Aggregation, Congestion Management, Feasible Operation Region, TSO-DSO Coordination, Approximate Dynamic Programming**

I. Introduction

With the increasing amount of renewable energy sources, congestions and voltage bound violations are more likely to occur. At the same time, an increasing number of Distributed Energy Resources (DERs) can provide *flexibility*, i.e., the ability to deviate from their active and reactive power set points within certain bounds. This property can be leveraged to mitigate congestions and voltage bound violations. From the Transmission System Operator's (TSO) perspective, the increasing number of DERs calls for methods towards structured flexibility aggregation to avoid the explicit consideration of a large amount of DER at the TSO level, and to prevent the communication of sensitive customer data.

There exist several approaches to estimate flexibility at the vertical interconnection to the upper-level grid [1–10]. These approaches compute an approximation of the set of admissible operating conditions of active and reactive power called *Feasible Operating Region (FOR)* via sampling. These samples approximate the FOR, e.g., by taking their convex hull. In general, however, it is not guaranteed that the FOR is convex due to the nonlinearity of the power flow equations [4]. Hence, calculating the convex hull may lead to the inclusion of points incompatible with technical limits and, therefore, to infeasibility of the disaggregation problem. In general, providing guarantees on the feasibility of aggregation-disaggregation schemes seems to be an open problem in the available literature.

In existing works the cost of DER usage is rarely considered in aggregation. The work [4, 8] compute level-sets for the DER cost via sampling. This results in a piece-wise defined cost function for the aggregated flexibility, which is cumbersome to consider in optimization at the TSO level.

In the present work, we approach aggregation in the framework of Approximate Dynamic Programming (ADP). ADP provides a powerful abstraction, leading to new avenues for flexibility and cost aggregation with feasibility guarantees [11]. From the ADP perspective, aggregation is a set projection problem that, for grid models constituting affine constraints, can be solved via tools from computational geometry [12] while avoiding the sampling efforts of existing methods. To guarantee affine presentation of the power flow equations, we utilize different variants of `DistFlow`, which combine computational efficiency with the consideration of voltage and current limits for radial grids [13]. Moreover, we employ the `DistFlow` variant from [14] to compute a strict inner approximation of the FOR to ensure feasibility. For heavily-loaded cases, the FOR critically depends on the voltage at the coupling node [15]. We show that our proposed scheme can easily incorporate this dependency. Furthermore, we propose a cost approximation that is easy to communicate and to integrate into numerical optimization schemes at the TSO level.

The paper is organized as follows: In Section II we present the TSO-DSO coordination problem and we review the state-of-the-art of flexibility aggregation. Section IV introduces our ADP framework, which we use in Section V to derive numerical aggregation methods based on different affine grid models. In Section VI, we propose a cost approximation scheme. We conclude our work in Section VII.

This research is supported by the German Federal Ministry for Economic Affairs and Climate Action (BMWK) under agreement no. 03EI4043A (Redispatch3.0).
Submitted to the 23rd Power Systems Computation Conference (PSCC 2024).

II. Problem Formulation

We briefly recall a basic AC Optimal Power Flow (OPF) problem for the combined TSO-DSO grid, which we use as a basis for our aggregation schemes [7, 16, 17].

A. AC Optimal Power Flow

Consider a power system described by a graph $G^e = (\mathcal{N}, \mathcal{B})$, where $\mathcal{N} = \{1, \dots, |\mathcal{N}|\}$ is the set of all buses in all voltage levels of the grid and $\mathcal{B} \subseteq \mathcal{N} \times \mathcal{N}$ is the set of branches. Assume that we have a balanced grid and zero line-charging capacitances. The associated bus-admittance matrix $Y = G + jB \in \mathbb{C}^{|\mathcal{N}|\times|\mathcal{N}|}$ is given by

$$[Y]_{k,l} = \begin{cases} \sum_{k\in\mathcal{N}} y_{k,l} & \text{if} \quad k = l, \\ -y_{k,l}, & \text{if} \quad k \neq l. \end{cases}$$

Here, $y_{k,l} = g_{k,l} + jb_{k,l} \in \mathbb{C}$ is the admittance of branch $(k,l) \in \mathcal{B}$, and $g_{k,l}$ and $b_{k,l}$ are its susceptance and conductance, respectively. Note that $y_{k,l} = 0$ if $(k,l) \notin \mathcal{B}$. The flow of active power and reactive power along branch $(k,l) \in \mathcal{B}$ is given by

$$p_{k,l} = v_k v_l (G_{k,l}\cos(\theta_{k,l}) + B_{k,l}\sin(\theta_{k,l})), \tag{1a}$$
$$q_{k,l} = v_k v_l (G_{k,l}\sin(\theta_{k,l}) - B_{k,l}\cos(\theta_{k,l})). \tag{1b}$$

Here, v_k is the voltage magnitude at node $k \in \mathcal{N}$ and $\theta_{k,l} \doteq \theta_k - \theta_l$ is the voltage angle difference between the two nodes $k, l \in \mathcal{N}$. Using (1), the AC power flow equations for all buses $k \in \mathcal{N}$ read

$$p_k = \sum_{l\in\mathcal{N}} p_{k,l}, \qquad q_k = \sum_{l\in\mathcal{N}} q_{k,l}, \tag{2}$$

where $p_k, q_k \in \mathbb{R}$ are the net active and reactive power injection at node $k \in \mathcal{N}$. These net powers are given by

$$p_k = p_k^g - p_k^d, \qquad q_k = q_k^g - q_k^d, \tag{3}$$

where p_k^g and q_k^g are the active/reactive power generation and p_k^d and q_k^d are the active/reactive power demand at node $k \in \mathcal{N}$. The active/reactive power generation must stay within lower and upper bounds

$$\underline{p}_k^g \leq p_k^g \leq \bar{p}_k^g, \qquad k \in \mathcal{G}. \tag{4}$$

For "flexible" renewable generators, i.e., generators which can alter their set points, we have $\underline{p}_k^g = 0$ and $\bar{p}_k = f_k^g$, where f_k^g represents the maximal active power generation given by irradiation/wind conditions. Moreover, the renewable generators $k \in \mathcal{G}$ are able to offer reactive power support q_k, constrained by the maximum apparent power $\bar{s}_k$ and a power factor limit α. Thus, we consider affine constraints [18]

$$p_k^g \leq \bar{s}_k \cos(\alpha), \quad -p_k \leq \alpha q_k \leq p_k. \tag{5}$$

The resulting optimization problem minimizes operation costs $f_k : \mathbb{R} \to \mathbb{R}$ while avoiding grid congestion

$$\min_x \sum_{k\in\mathcal{G}} f_k(p_k^g)$$
$$\text{subject to} \quad \text{(1)-(5)}, \tag{6a}$$
$$\underline{v} \leq v_k \leq \bar{v}, \qquad k \in \mathcal{N}, \tag{6b}$$
$$p_{k,l}^2 + q_{k,l}^2 \leq \bar{s}_{k,l}^2, \qquad (k,l) \in \mathcal{B}, \tag{6c}$$
$$p_k^g = q_k^g = 0, \qquad k \in \mathcal{N} \setminus \mathcal{G}, \tag{6d}$$
$$\theta_1 = 0, \quad v_1 = 1, \tag{6e}$$

Here, (6b) and (6c) express the voltage and line limits. The feasible set of problem (6) reads

$$\mathcal{X}^{\mathrm{AC}} \doteq \left\{ x \in \mathbb{R}^{n_x} \mid \text{(6a)-(6e) hold } \forall k \in \mathcal{N}, \text{ and } \forall (k,l) \in \mathcal{B} \right\}$$
$$\text{with } x \doteq \left[[p_k^g, q_k^g, p_k, q_k, v_k, \theta_k]_{k\in\mathcal{N}}, [p_{k,l}, q_{k,l}]_{(k,l)\in\mathcal{B}}^\top \right].$$

III. The Aggregation Problem and Established Solution Approaches

Problem (6) is generally hard to solve across multiple voltage levels and system operators. To reduce complexity, aggregation approaches can exploit the natural tree structure among TSOs and DSOs systems, cf. Figure 2.

A. Problem Partitioning

We decompose the set of buses $\mathcal{N}$ into a set with the TSO buses $\mathcal{N}_1$ and into $|\mathcal{C}|$ bus sets for the DSOs $\mathcal{N}_i, i \in \mathcal{C}$, for all DSOs where $\mathcal{C} \doteq \{2, \dots, |\mathcal{S}|\}$. Similarly, we split the set of branches $\mathcal{B}$ into $\{\mathcal{B}_i\}_{i\in\mathcal{S}}$ such that all branches connecting nodes in $\mathcal{N}_i$ belong to $\mathcal{B}_i$. We assign the branches connecting TSO and DSO grids $\mathcal{B}_i^c \subseteq \mathcal{B}_i$ to the DSOs. We denote the buses at the TSO level connected to a branch between TSO and DSO i as $\mathcal{N}_i^c \subseteq \mathcal{N}$.

With the above definitions, one obtains local constraint sets

$$\mathcal{X}_i^{\mathrm{AC}} \doteq \left\{ x_i \in \mathbb{R}^{n_{xi}} \mid \text{(6a)-(6d) hold } \forall k \in \mathcal{N}_i, \text{ and } \forall (k,l) \in \mathcal{B}_i \right\}$$

where $x_i \doteq \left[[p_k^g, q_k^g, p_k, q_k, v_k, \theta_k]_{k\in\mathcal{N}_i}, [p_{k,l}, q_{k,l}]_{(k,l)\in\mathcal{B}_i}^\top \right]$ for all $i \in \mathcal{C}$. The TSO set $\mathcal{X}_1$ is defined as above with the additional reference constraints (6e).

We distinguish between *local variables* $\{y_i\}_{i\in\mathcal{C}\cup\{1\}}$ and *coupling variables* $\{z_{ij}\}_{i,j\in\mathcal{S}\cup\{1\}}$, where we define local variables of subsystem $i \in \mathcal{S}$ as all variables on which only one f_i or $\mathcal{X}_i$ depend. Since we assume a tree structure between the system operators, each child (DSO) has a unique parent (TSO). Thus, we define $z_i \doteq z_{i,\mathrm{par}(i)}$ as the coupling variable of DSO $i \in \mathcal{S}$ with the TSO. For the sake of simplicity, we avoid a more formal description of the underlying interaction graph and instead refer to [11] for details.

Next, we identify coupling variables of problem (6). Consider the power flow equations (1) for coupling lines $(k,l) \in \mathcal{B}_i^c$ in combination with nodal power balance (2) for coupling nodes $k \in \mathcal{N}_i^c$ in Figure 1. Doing so reveals that coupling variables are $z_i^\top \doteq$

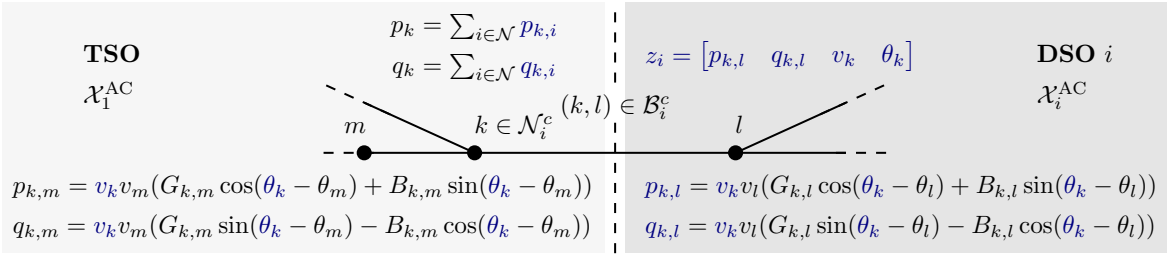

Fig. 1: Coupling variables z_i (blue) between the constraint set of the TSO $\mathcal{X}_1^{\mathrm{AC}}$, and one DSO constraint set $\mathcal{X}_i^{\mathrm{AC}}$ for $(k,l) \in \mathcal{B}_i^c$.

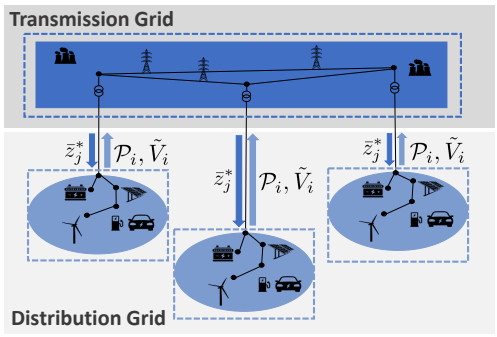

Fig. 2: Hierarchically structured power system.

$\left[[p_{k,l}, q_{k,l}]_{(k,l)\in\mathcal{B}_i^c}, [v_k, \theta_k]_{k\in\mathcal{N}_i^c}\right]$, and local decision variables are $y_i^\top \doteq \left[[p_k^g, q_k^g, p_k, q_k]_{k\in\mathcal{N}_i}, [v_k, \theta_k]_{k\in\mathcal{N}_i\setminus\mathcal{N}_i^c}^\top, [p_{k,l}, q_{k,l}]_{(k,l)^\top\in\mathcal{B}_i\setminus\mathcal{B}_i^c}^\top\right]$ for all $i \in \mathcal{C}\cup\{1\}$.

Using the above, the *aggregation problem from the TSO perspective* can be phrased as follows:

Determine all values of coupling variables z_i, that can be generated using the flexibility of DERs in the distribution grids.

Note that this formulation is generic: it is equivalently applicable to multi-stage OPF including storage and to problems with multiple interconnections to the upper-level grid. In these cases, the constraints included in $\mathcal{X}_i$ and the dimension of z_i changes.

B. Existing Approaches

Observe that the feasible set of the DSO sub-problems $\mathcal{X}_i^{\mathrm{AC}}$ contain the power flow equations (1)-(3) and (6d) as equality constraints. For fixed set-points of the flexibilities $(p_k^g, q_k^g)_{k\in\mathcal{N}_i}$ in the DSO grid, these equations can be solved uniquely for the corresponding coupling variables z_i solving a power flow problem. Early approaches sample $(p_k^g, q_k^g)_{k\in\mathcal{N}_i}$ (e.g., from uniform distributions) and compute the corresponding z_i numerically for a fixed $v_k = 1$ at the interconnection $k \in \mathcal{N}_i^c$ [1, 3, 5, 6]. Points that do not satisfy the inequality constraints ((4),(5),(6a),(6b)) are neglected a posteriori. This leads to a collection of feasible points for z_i, i.e., for a set of admissible $\{p_{k,l}, q_{k,l}\}_{(k,l)\in\mathcal{B}_i^c}$ at the interconnection to the TSO grid.

More recent approaches explore the boundary of admissible z_i more systematically by solving a sequence of auxiliary optimization problems

$$\min_{y_i, z_i} \sum_{(k,l)\in\mathcal{B}_i^c} c_{k,l}\, p_{k,l} + d_{k,l}\, q_{k,l} \quad \text{s.t.} \quad (y_i, z_i) \in \mathcal{X}_i^{\mathrm{AC}}, \tag{7}$$

where $c_{k,l}, d_{k,l} \in \{-1, 0, 1\}$ are cost coefficients. Note that the solution to (7), $(p_{k,l}^\star, q_{k,l}^\star)$, is located at the boundary of $\mathcal{P}_i^{\mathrm{AC}}$, see also [2, 7, 8].

The above methods compute sampling points, which are difficult to consider in the TSO problem without further processing. A common remedy is to compute the convex hull of the sampling points leading to a convex polyhedron, which can be easily integrated into the TSO problem. This polyhedron is, however, an approximation of the true admissible set and thus might include non-admissible $\{p_{k,l}, q_{k,l}\}_{(k,l)\in\mathcal{B}_i^c}$, cf. Section V-C. If the TSO chooses one of these points values, disaggregation fails.

IV. Aggregation via Approximate Dynamic Programming

The aggregation ideas from above can be generalized to tree-structured optimization problems resulting in Feasibility-Preserving Approximate Dynamic Programming (FP-ADP) [11]. Next, we apply this ADP framework to problem (6).

A. Aggregation as Set Projection

The fundamental observation of FP-ADP is that aggregation is equivalent to a set projection of the feasible set of the DSOs, $\mathcal{X}_i$, on the coupling variables z_i. The *set projection* of $\mathcal{X} \subseteq \mathcal{Y}\times\mathcal{Z}$ onto $\mathcal{Z}$ is defined as [19]

$$\mathrm{proj}_{\mathcal{Z}}(\mathcal{X}) \doteq \{z \in \mathcal{Z} \mid \exists\, y \in \mathcal{Y} \text{ with } (z,y) \in \mathcal{X}\} \subseteq \mathcal{Z}. \tag{8}$$

The above definition (8) can be interpreted as searching for all coupling variables to the TSO, z_i, for which there exist local variables y_i, i.e., admissible set-points of the local DERs, which satisfy all grid constraints. Hence, aggregation can be interpreted as computing the FOR

$$\mathcal{P}_i^{\mathrm{AC}} \doteq \mathrm{proj}_{\mathcal{Z}_i} \mathcal{X}_i^{\mathrm{AC}}. \tag{9}$$

B. Value-Function Reformulation

Next, we outline the full loop of aggregation, solving the TSO problem, and disaggregation in the framework of FP-ADP [11]. Doing so allows to guarantee feasibility and it enables to include cost information in the aggregation-disaggregation scheme.

We partition the cost function of problem (6) into local ones

$$f_i(x) \doteq \sum_{k \in \mathcal{G}_i} f_k(p_k^g), \tag{10}$$

where $\mathcal{G}_i$ is the set of generators in DSO problem $i \in \mathcal{C}$. Next, we reformulate problem (6) via value-functions V_i for each DSO, which depend on the coupling variables z_i:

$$\min_{y_1, \{z_j\}_{j \in \mathcal{C}}} f_1(y_1) + \sum_{j \in \mathcal{C}} V_j(z_j) \tag{11a}$$

$$\text{subject to } (y_1, \{z_j\}_{j \in \mathcal{C}}) \in \bar{\mathcal{X}}_1^{\mathrm{AC}}. \tag{11b}$$

Recall that $\mathcal{C}$ is the set of all DSOs, and subsystem $j = 1$ refers to the TSO. Moreover,

$$\bar{\mathcal{X}}_1 \doteq \mathcal{X}_1 \cap (\mathbb{R}^{n_{y1}} \times \bigcap_{j \in \mathcal{C}} \mathcal{P}_j^{\mathrm{AC}}),$$

where $\mathcal{X}_1$ is the constraint set of the TSO and $\mathcal{P}_i^{\mathrm{AC}}$ is the set projection of the feasible sets of the DSO problems onto the coupling variables with its parent z_i from (9), i.e., the FOR of the feasible sets of all DSOs.

The value functions V_j are defined via *DSO problems*

$$V_i(z_i) \doteq \min_{y_i} f_i(y_i, z_i) \tag{12a}$$

$$\text{subject to } (y_1, z_i) \in \mathcal{X}_i^{\mathrm{AC}} \tag{12b}$$

for all $i \in \mathcal{C}$. Note that V_i includes cost information of the DSOs, i.e., the cost for using a DER can be communicated to the TSO via V_i. Computing V_i explicitly is hard in general due to the minimization over y_i. An explicit computation is possible only for special problem classes such as convex quadratic programs [20]. To overcome this issue, one can compute approximations $\tilde{V}_i \approx V_i$, one of which we present in Section VI.

C. Feasibility-Preserving ADP

The overall algorithm is summarized in Algorithm 1 with a graphical illustration in Figure 2. In step 1), the projections $\mathcal{P}_i^{\mathrm{AC}}$ (i.e., the FORs) of the feasible sets of all DSO problems $j \in \mathcal{C}$ are computed (Aggregation). It is possible to combine this information with an approximation of the value function $\tilde{V}_i \approx V_i$ which captures cost information. If this is not desired, one can use the trivial approximation $\tilde{V}_i \equiv 0$ or the approximation presented in Section VI. Step 2) includes all $(\mathcal{P}_i^{\mathrm{AC}}, \tilde{V}_i)$ in the TSO problem (11), which is solved in step 3). The optimal coupling variables $\bar{z}_i^\star$, are communicated to the DSOs in step 4). The DSOs solve their OPF problems (12) for fixed $\bar{z}_i^\star$ (Disaggregation) in Step 5).

Note that if one is able to compute exact projections $\mathcal{P}_i^{\mathrm{AC}}$ and exact value functions V_i, Algorithm 1 recovers the exact solution of the original OPF problem (6). Moreover,

Algorithm 1: Feasibility-Preserving ADP for (6)

Backward sweep:
1) Compute the FORs $\mathcal{P}_i^{\mathrm{AC}}$ via (9), and $\tilde{V}_i \approx V_i$ for all DSOs $i \in \mathcal{C}$ and send them to the TSO. *(Aggregation)*
2) Include all $(\tilde{V}_i, \mathcal{P}_i^{\mathrm{AC}})$ into the TSO problem (11).

Forward sweep:
3) Solve (11). *(Solve TSO problem)*
4) Distribute optimal coupling variables $\bar{z}_j^\star$ to all DSOs $j \in \mathcal{C}$.
5) Solve (12) for fixed $\bar{z}_j^\star$ at all DSOs. *(Disaggregation)*

if we replace V_i with approximations $\tilde{V}_i$ and compute $\mathcal{P}_i^{\mathrm{AC}}$ by suitable, i.e., not too conservative, inner approximations $\tilde{\mathcal{P}}_i \subseteq \mathcal{P}_i^{\mathrm{AC}}$, Algorithm 1 guarantees to compute a feasible but potentially sub-optimal solution [11]. Recall that for a safe system operation, guaranteed feasibility is pivotal.

V. Aggregation Based on Set Projection

The previous discussion leads to four *core research questions* for aggregation:

1) How to efficiently compute set projections $\mathcal{P}_i^{\mathrm{AC}}$ or approximations thereof ($\tilde{\mathcal{P}}_i \approx \mathcal{P}_i^{\mathrm{AC}}$)?
2) How to ensure that approximations satisfy $\tilde{\mathcal{P}}_i \subseteq \mathcal{P}_i^{\mathrm{AC}}$?
3) What are suitable value function surrogates $\tilde{V}_i \approx V_i$ that capture the cost of DER usage?
4) What are suitable parametrizations and data formats to communicate $(\mathcal{P}_i^{\mathrm{AC}}, V_i)$ between DSOs and the TSO?

In the following, we present first ideas for addressing these questions. We focus on the computation of the projections $\mathcal{P}_i^{\mathrm{AC}}$ and $\tilde{\mathcal{P}}_i$, i.e., on aggregation, which is most expensive and critical in Algorithm 1 to guarantee feasibility of solutions.

All numerical results in this section are based on the 15-bus radial DSO grid model `case15nbr` from [21, 22], where the loads on buses $8, 10$ and 13 are replaced by renewable generators with double the active power limit. We use `JuMP` and `IPOPT` for solving optimization problems and `Polyhdra.jl` for computing polyhedral projections [23–25]. The computations used an Intel i5-10210U machine with $8\,\mathrm{GB}$ of RAM.

We start by assuming constant voltage $v_k = 1\,\mathrm{p.u.}$ for the coupling node $k \in \mathcal{N}_i^c$ as commonly done in the literature. Since this assumption might not always be satisfied in reality, we show how to consider voltage dependency in our scheme later in Section V-E. Furthermore, we use a quadratic penalization of RES curtailment for a cost f_k.

A. Projection Based on the DC Model

In case the DC model is used for the DSO problems, $\mathcal{X}_i$ is a convex polyhedron in half-space representation (H-polyhedron) [12, 26]

$$\mathcal{X}_i^{\mathrm{DC}} \doteq \{x_i \mid A_i x_i = b_i,\ C_i x_i \leq d_i\},$$

where the matrices and vectors (A_i, C_i, b_i, d_i) contain the DC power flow equations, generator limits and line flow

limits [11]. In this case, projection algorithms from computational geometry such as Fourier-Motzkin elimination or vertex enumeration can be used to compute $\mathcal{P}_i^{\mathrm{DC}}$, cf. [26–28] and references therein for an overview, and to [29] for an implementation. However, using the DC model for distribution grid is problematic since voltage limits and the reactive power are neglected. Furthermore, the feasible range in the active power can be too optimistic since line losses are neglected. Next, we employ different versions of the `DistFlow` model for radial and balanced grids, which allows constraining nodal voltage magnitudes and reactive power. These constraints are especially important for distribution grid operation.

B. Projection Based on the DistFlow Model

Consider the `DistFlow` model [30]—an alternative representation to the AC power flow model for radial grids. It reads

$$p_{k,l} = \sum_{j \in \mathcal{C}_k} p_{k,j} + p_k + r_{k,l}\, \ell_{k,l}, \tag{13a}$$

$$q_{k,l} = \sum_{j \in \mathcal{C}_k} q_{k,j} + q_k + x_{k,l} \ell_{k,l}, \tag{13b}$$

$$\nu_k = \nu_l + 2(r_{k,l}\, p_{k,l} + x_{k,l}\, q_{k,l}) - (r_{k,l}^2 + x_{k,l}^2)\ell_{k,l}, \tag{13c}$$

$$\ell_{k,l} = \frac{p_{k,l}^2 + q_{k,l}^2}{\nu_l} \tag{13d}$$

where $r_{k,l}$ and $x_{k,l}$ are the resistance and reactance, the real and imaginary part of the impedance $z_{k,l} = \frac{1}{g_{k,l}+jb_{k,l}}$ of branch $(k,l) \in \mathcal{B}$. The variables ν_k and $\ell_{k,l}$ are, respectively, the squared nodal voltage and the squared branch current, i.e.,

$$\nu_k \doteq v_k^2 \quad \text{for all} \quad k \in \mathcal{N}. \tag{14}$$

Hence, the feasible set of the DSO problems becomes

$$\mathcal{X}_i^{\mathrm{DF}} \doteq \big\{x_i \in \mathbb{R}^{n_{xi}} \mid \text{(2)-(5), (6b)-(6d), and (13) hold for all } k \in \mathcal{N}_i, \text{ and } \forall (k,l) \in \mathcal{E}_i\big\},$$

with $x_i = \Big[[p_k^g, q_k^g, p_k, q_k, v_k, \theta_k]_{k\in\mathcal{N}_i}, [p_{k,l}, q_{k,l}]_{(k,l)\in\mathcal{B}_i}^\top\Big]$. Note that $\mathcal{X}_i^{\mathrm{DF}}$ and $\mathcal{X}_i^{\mathrm{AC}}$ are equivalent under a nonlinear coordinate transformation, i.e., $\mathcal{X}_i^{\mathrm{DF}}$ is (in contrast to the following models) *not* an approximation.

C. Approximation via LinDistFlow and Loss Linearization

The only constraint leading to non-convexity of the `DistFlow` model is (13d). Hence, different simplifications of the equation have been proposed in the literature. In the simplest version, [13], `LinDistflow`, line impedances are neglected and therefore the squared branch current $\ell_{k,l}$ is taken out of the calculation of power branches and nodal voltages, i.e., $\ell_{k,l} = 0$. Unlike the DC formulation, `LinDistFlow` also models non-constant voltages. The resulting set of constraints

$$\begin{aligned}
\mathcal{X}_i^{\mathrm{LDF}} = \; & \{x_i \in \mathbb{R}^{n_{xi}} \mid \text{(3)-(5), (13a)} - \text{(13c)}, && \text{(15a)}\\
& \underline{v}^2 \le \nu_k \le \bar{v}^2, && k \in \mathcal{N}_i, && \text{(15b)}\\
& p_k^g = q_k^g = 0, && k \in \mathcal{N}_i \setminus \mathcal{G}_i, && \text{(15c)}\\
& \ell_{k,l} = 0, && (k,l) \in \mathcal{B}_i\} && \text{(15d)}
\end{aligned}$$

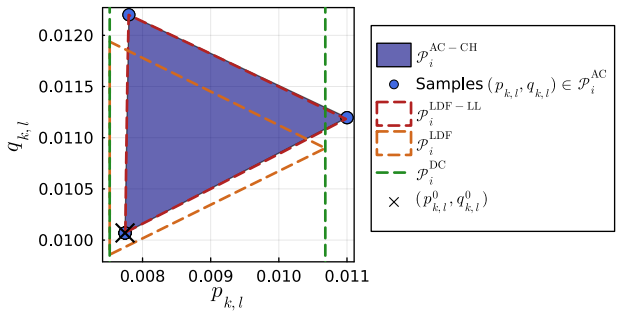

Fig. 3: Computing $\mathcal{P}_i^{\mathrm{AC}}$ using set projection.

has only affine terms and is thus again a H-polyhedron. The resulting projection on the coupling variables (aggregation) is shown in Figure 3 (orange). Furthermore, Figure 3 shows the "true" $\mathcal{P}_i^{\mathrm{AC}}$ computed with sufficiently fine sampling from Section III-B, and its corresponding convex hull $\mathcal{P}_i^{\mathrm{AC-CH}}$.

We can see that the $\mathcal{P}_i^{\mathrm{LDF}} \doteq \mathrm{proj}_{\mathcal{Z}_i}\left(\mathcal{X}_i^{\mathrm{LDF}}\right)$ using `LinDistFlow` approximates $\mathcal{P}_i^{\mathrm{AC}}$ relatively well, but the center is off-set compared to $\mathcal{P}_i^{\mathrm{AC}}$ to the lower left. This is due to the fact that `LinDistFlow` neglects the power losses, which results in the underestimation of the required power at the interconnection to satisfy the demand.

Loss Linearization: Replacing (15d) by an affine approximation mitigates this issue. Here, similarly to [14, 31, 32], we approximate (13d) by

$$\ell_{k,l} \approx \ell_{k,l}^0 + J_{k,l}|_{x_{k,l}^0}^\intercal\, \delta_{k,l} \tag{16}$$

where

$$\delta_{k,l} = \begin{bmatrix} p_{k,l} - p_{k,l}^0 \\ q_{k,l} - q_{k,l}^0 \\ \nu_l - \nu_l^0 \end{bmatrix}, J_{k,l}|_{x_{k,l}^0} = \begin{bmatrix} \frac{2p_{k,l}}{\nu_l^0} \\ \frac{2q_{k,l}}{\nu_l^0} \\ -\frac{(p_{k,l}^0)^2 + q_{k,l}^0)^2}{(\nu_l^0)^2} \end{bmatrix}, \tag{17}$$

i.e., its first order Taylor series around the current operation point $x_{k,l}^0 \doteq [p_{k,l}^0, q_{k,l}^0, \nu_l^0]$ for all $(k,l) \in \mathcal{E}$.

This leads to

$$\mathcal{X}_i^{\mathrm{LDF-LL}}(x_i^0) \doteq \big\{x_i \in \mathbb{R}^{n_{xi}} \mid \text{(15a)-(15c), (16)}\big\}, \tag{18}$$

which is again a convex polytope.

The resulting $\mathcal{P}_i^{\mathrm{LDF-LL}}$ of the `LinDistFlow` is also shown in Figure 3 (red). Although not being an inner approximation of $\mathcal{P}_i^{\mathrm{AC}}$, $\mathcal{P}_i^{\mathrm{LDF-LL}}$ is a close approximation computed in one step, i.e., avoiding solving multiple AC OPF problems. Moreover, it explicitly maintains (close to) feasibility in the current and voltage limits of the DSO grid.

Extreme Renewable Generation: Next, we analyze the approximation using the different methods in an extreme case, when the power generation is unrealistically high. Figure 4 shows the results of this experiment. We can see that calculating the convex hull of the sampled points using the AC-OPF leads to the inclusion of infeasible points, since the area is non-convex.

The projection using the DC model no longer provides

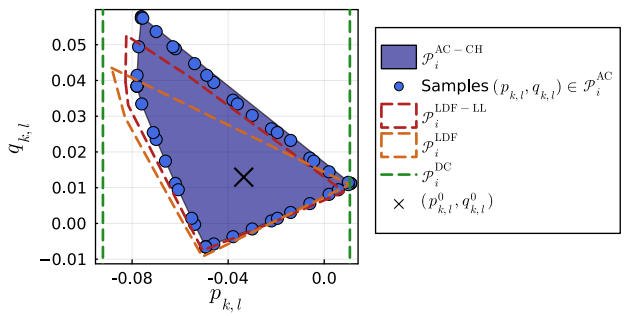

Fig. 4: Approximations of $\mathcal{P}_i^{\mathrm{AC}}$ using set projection for extremely high generation.

the same range for active power as the `LinDistFlow` model. This is due to the fact that the DC model doesn't express the nodal voltages and cannot therefore identify the voltage violation that may occur. The `LinDistFlow` model considers the voltages, but by ignoring the losses it still overestimate the active power range. Lastly, we can see that the `LDF-LL` variant suffers from the much larger range of flexibility, having a worst approximation in the areas further away from the operational point.

D. Inner Approximation of DistFlow Based on [14]

Another challenge is to compute "true" inner approximations $\tilde{\mathcal{P}}_i \subseteq \mathcal{P}_i^{\mathrm{AC}}$. Next, we present an approach based on [14], which seems to deliver that for our setting although this is not proven yet. The key idea is to replace (13d), with lower and upper bounds instead of linearizations

$$\begin{aligned}\ell_{k,l}(\delta^+,\delta^-;x^0) &\le \ell_{k,l}^+ \\ &\doteq \ell_{k,l}^0 + \max\{2|J_{k,l+}^\intercal \delta_{k,l}^+ + J_{k,l-}^\intercal \delta_{k,l}^-|, \Psi_{k,l}\}, \quad (19a)\\ \ell_{k,l}(\delta^+,\delta^-;x^0) &\ge \ell_{k,l}^- \doteq \ell_{k,l}^0 + J_{k,l+}^\intercal \delta_{k,l}^- + J_{k,l-}^\intercal \delta_{k,l}^+, \quad (19b)\end{aligned}$$

where

$$H_{k,l}|_{x_{k,l}^0} = \begin{bmatrix} \frac{2}{\nu_l^0} & 0 & -\frac{2p_{k,l}}{(\nu_l^0)^2} \\ 0 & \frac{2}{\nu_l^0} & -\frac{2q_{k,l}}{(\nu_l^0)^2} \\ -\frac{2p_{k,l}}{(\nu_l^0)^2} & -\frac{2q_{k,l}}{(\nu_l^0)^2} & 2\frac{(p_{k,l}^0)^2+q_{k,l}^0)^2}{(\nu_l^0)^3} \end{bmatrix}, \quad (20a)$$

where $J_{k,l+}$ ($J_{k,l-}$) are vectors in which only the positive (negative) elements of $J_{k,l}$ appear and the other elements are 0 and $\Psi_{k,l}$ represents the maximum value obtained by evaluating $(\delta_{k,l}^{+/-})^\intercal H_{k,l}|_{x_{k,l}^0}(\delta_{k,l}^{+/-})$ over eight different combinations of $\delta_{k,l}^{+/-}$. These combinations arise from considering the two possibilities for each of the three elements ($p_{k,l}$, $q_{k,l}$, v_k), switching the lower and upper bound for $\ell_{k,l}$ in the calculation, described below in (21a)-(21f), cf. [14]. With these bounds, we define proxy variables

$$\begin{aligned} p_{k,l}^+ &\ge \sum_{j\in\mathcal{C}_k} p_{k,j} - p_k + r_{k,l}\ell_{k,l}^+(\delta^+,\delta^-;x^0), && (21a)\\ p_{k,l}^- &\doteq \sum_{j\in\mathcal{C}_k} p_{k,j} - p_k + r_{k,l}\ell_{k,l}^-(\delta^+,\delta^-;x^0), && (21b)\\ q_{k,l}^+ &\ge \sum_{j\in\mathcal{C}_k} q_{k,j} - q_k + x_{k,l}\ell_{k,l}^+(\delta^+,\delta^-;x^0), && (21c)\\ q_{k,l}^- &\doteq \sum_{j\in\mathcal{C}_k} q_{k,j} - q_k + x_{k,l}\ell_{k,l}^-(\delta^+,\delta^-;x^0), && (21d)\\ \nu_k^+ &\doteq \nu_l - 2r_{k,l}p_{k,l}^- - 2x_{k,l}q_{k,l}^- + (r_{k,l}^2+x_{k,l}^2)\ell_{k,l}^+(\cdot), && (21e)\\ \nu_k^- &\doteq \nu_l - 2r_{k,l}p_{k,l}^+ - 2x_{k,l}q_{k,l}^+ + (r_{k,l}^2+x_{k,l}^2)\ell_{k,l}^-(\cdot). && (21f)\end{aligned}$$

The idea is that these proxy variables represent the "worst case" for their counterparts by assuming that the corresponding term for $\ell_{k,l}$ is fixed at its lower/upper bound. Since $r_{k,l}, x_{k,l} \ge 0$, these variables satisfy

$$p_{k,l}^- \le p_{k,l} \le p_{k,l}^+, \quad q_{k,l}^- \le q_{k,l} \le q_{k,l}^+, \quad \nu_k^- \le \nu_k \le \nu_k^+, \quad (22)$$

where $(p_{k,l}, p_{k,l}, \nu_k)$ are the "true" values from (13). If we require that these proxy variables satisfy

$$\begin{aligned} \underline{v} \le v_k^-, \qquad v_k^+ \le \bar{v}, \qquad & k \in \mathcal{N}, && (23a)\\ 0 \le l_{k,l}^-, \qquad l_{k,l}^+ \le \bar{l}_{k,l}, \qquad & (k,l) \in \mathcal{B}, && (23b)\end{aligned}$$

we get ranges for the admissible z_i for fixed set-points of the DERs which correspond to the uncertainty due to the absence of exact knowledge of the loss term. Consider

$$\mathcal{X}_i^{\mathrm{DF+}} \doteq \{(p^-, p, p^+, q^-, q, q^+, \nu^-, \nu, \nu^+) \mid (19)\text{-}(23) \text{ holds}\},$$

which is an enlarged feasible set based on the `DistFlow` model including all proxy variables. Observe that $\mathcal{X}_i^{\mathrm{DF+}}$ is convex but described by nonlinear inequalities due to (19a). Hence, we can *not* use the polyhedral tools from before.

However, we can use the sampling-based approach from Section III-B, where we replace the feasible set by $\mathcal{X}_i^{\mathrm{DF+}}$. Doing so yields a range of possible $(p_{k,l}, q_{k,l}), (k,l) \in \mathcal{B}_i^c$ defined by their corresponding proxy variables, see Figure 5 (yellow boxes). The uncertainty in $(p_{k,l}, q_{k,l}), (k,l) \in \mathcal{B}_i^c$ comes from the unknown losses, which are considered via the upper and lower bounds (19). We compute the corresponding $\mathcal{P}_i^{\mathrm{DF+}}$ (Figure 5 (green)) set as the intersection of all $\tilde{\mathcal{P}}_i^{\mathrm{DF+}}$, i.e, the four polyhedra formed by the sampling of the different proxy variables (p^-, q^-), (p^-, q^+), (p^+, q^-), (p^+, q^+). It is intuitively clear that this corresponds to feasibility even in the worst realization of the losses and we conjecture that doing so leads to an inner-approximation $\mathcal{P}_i^{\mathrm{DF+}} \subseteq \mathcal{P}_i^{\mathrm{AC}}$. Numerical simulations support this conjecture; a rigorous proof is, however, subject to future investigation. Observe that around the operational point, Figure 5 (black cross), the difference between over and under approximation of the loss is small. The opposite is true for points far from x^0 indicating a high dependency of the tightness of the approximation on the operation point.

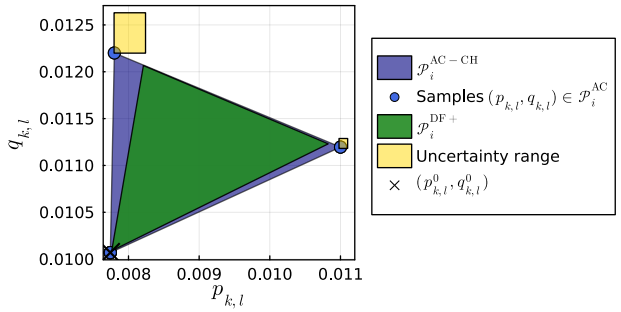

Fig. 5: Inner approximation of $\mathcal{P}_i^{\mathrm{AC}}$.

E. Considering Voltage Dependency

Now, we demonstrate the influence of the voltage on the FOR and show that the proposed method can include voltage information easily. Figure 6a shows $\mathcal{P}_i^{\mathrm{LDF}}$, where the voltage is not fixed anymore. One can see that if there is no congestion on the lower grid, it is reasonable to fix the voltage at the interconnection when calculation the aggregated area since the FOR for $p_{k,l}$ and $q_{k,l}$, $(k,l) \in \mathcal{B}_i^c$ almost doesn't change with a change in ν_k. However, considering that the main application scenario of flexibilities is in case of congestion and voltage bound violations, this assumption is not reasonable, cf. Figure 6b. It is also important to note that with our method it is relatively simple to represent this interdependence: we simply project the constraint set onto three variables instead of two.

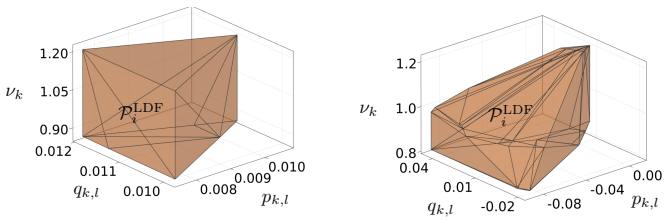

(a) Basic feed-in. (b) High feed-in.

Fig. 6: Dependency of $(p_{k,l}, q_{k,l})$ on ν_l, $(k,l) \in \mathcal{B}_i^c$.

F. Comparison

Computation times for all previous aggregation schemes are summarized in Table I. The computation time of the sampling approaches for $\mathcal{P}_i^{\mathrm{AC}}$ and $\mathcal{P}_i^{\mathrm{DF+}}$ via (7) depends on the number of samples, i.e., their desired "resolution". Sampling $\mathcal{P}_i^{\mathrm{DF+}}$ requires the highest amount of time due to the nonlinear model and the additional proxy variables. Projection of $\mathcal{P}_i^{\mathrm{LDF}}$ and $\mathcal{P}_i^{\mathrm{LDF-LL}}$ via `Polyhedral.jl` is slightly faster and projecting $\mathcal{P}_i^{\mathrm{DC}}$ shows the lowest computational time due to its simplicity. With respect to the quality of solution, the resulting $\mathcal{P}_i^{\mathrm{LDF-LL}}$ seems to deliver the closest approximation of $\mathcal{P}_i^{\mathrm{AC}}$. From the sampling methods, $\mathcal{P}_i^{\mathrm{DF+}}$ results in a convex inner-approximation of $\mathcal{P}_i^{\mathrm{AC}}$ potentially leading to feasibility guarantees. However, depending on the load, this approximation can be conservative and feasibility might be lost. The sampling of $\mathcal{P}_i^{\mathrm{AC}}$ in combination with the convex hull includes infeasible points, which can lead to failure of the overall scheme.

TABLE I: Computation times.

Algorithm	#Samples	Time (s)
AC Sampling of $\mathcal{P}_i^{\mathrm{AC}}$	18	0.626377
	64	1.624352
AC Sampling of $\mathcal{P}_i^{\mathrm{DF+}}$	18	2.532605
	64	6.197835
Projection $\mathcal{P}_i^{\mathrm{DC}}$	-	0.001840
Projection $\mathcal{P}_i^{\mathrm{LDF}}$	-	0.222937
Projection $\mathcal{P}_i^{\mathrm{LDF-LL}}$	-	2.927589

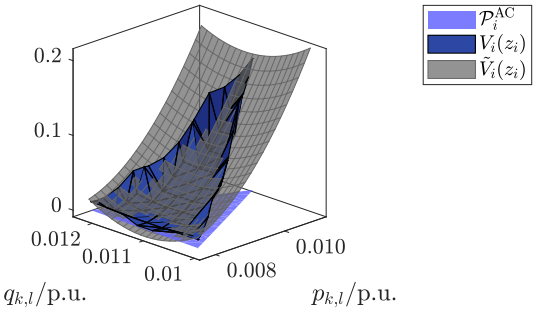

Fig. 7: Approximated cost of flexibility usage for $v_i = 1\,\mathrm{p.u.}$.

VI. Cost Aggregation

Often it is important to also communicate some cost information $\tilde{V}_i \approx V_i$ for DER usage such that the TSO can choose an economical set-point. Next, we present a quadratic fit for V_i, which can be easily communicated to the TSO via one matrix-vector tuple. This description is smooth and easy to handle by numerical solvers at the TSO level.

First, we collect samples of V_i, which we do by gridding. For each grid-point $\bar{z}_i = (\bar{p}_{k,l}, \bar{q}_{k,l})$ with $v_k = 1\,\mathrm{p.u.}$[1] at the interconnection $(k,l) \in \mathcal{B}_i^c$, we evaluate (12), i.e., we compute $V_i(\bar{z}_i)$ via numerical optimization. We then use a simple least-squares regression from `Optim.jl` [33] to fit a quadratic function

$$V_i(z_i) \approx \tilde{V}_i(z_i) \doteq \frac{1}{2} z_i^\top H_i z_i + h_i^\top z_i, \tag{24}$$

where (H_i, h_i) are the coefficients to be found. The resulting fit $\tilde{V}_i$ and the "true" V_i computed by interpolation of samples are shown in Figure 7. Although not being exact, especially close to the boundary of $\mathcal{P}_i^{\mathrm{AC}}$, the quadratic function provides a good approximation in the interior, which is valuable information for the TSO.

VII. Conclusion and Outlook

In this paper, we have proposed a framework for flexibility and cost aggregation based on approximate dynamic programming, which provides feasibility guarantees and makes established tools from computational geometry available for

[1] In contrast to the FOR $\mathcal{P}_i^{\mathrm{AC}}$, the cost V_i is insensitive to voltage change.

aggregation. We have implemented the framework using different versions of the `DistFlow` model on a medium-sized feeder. These results show that our proposed approach allows to capture voltage information and they demonstrate promising features of the proposed framework.

Future work will investigate rigorous inner approximation properties and the extension towards problems with multiple interconnections and including storage.

REFERENCES

[1] O. Krause, S. Lehnhoff, E. Handschin, Ch. Rehtanz, and H. F. Wedde, "On feasibility boundaries of electrical power grids in steady state," *International Journal of Electrical Power & Energy Systems*, vol. 31, no. 9, pp. 437–444, 2009.

[2] M. Kalantar-Neyestanaki, F. Sossan, M. Bozorg, and R. Cherkaoui, "Characterizing the Reserve Provision Capability Area of Active Distribution Networks: A Linear Robust Optimization Method," *IEEE Transactions on Smart Grid*, vol. 11, no. 3, pp. 2464–2475, 2020.

[3] D. Mayorga Gonzalez, J. Hachenberger, J. Hinker, F. Rewald, U. Häger, C. Rehtanz, and J. Myrzik, "Determination of the Time-Dependent Flexibility of Active Distribution Networks to Control Their TSO-DSO Interconnection Power Flow," in *2018 Power Systems Computation Conference (PSCC)*, 2018, pp. 1–8.

[4] M. Sarstedt and L. Hofmann, "Monetarization of the Feasible Operation Region of Active Distribution Grids Based on a Cost-Optimal Flexibility Disaggregation," *IEEE Access*, vol. 10, pp. 5402–5415, 2022.

[5] M. Sarstedt, L. Kluß, J. Gerster, T. Meldau, and L. Hofmann, "Survey and Comparison of Optimization-Based Aggregation Methods for the Determination of the Flexibility Potentials at Vertical System Interconnections," *Energies*, vol. 14, no. 3, p. 687, 2021.

[6] M. Heleno, R. Soares, J. Sumaili, R. Bessa, L. Seca, and M. A. Matos, "Estimation of the flexibility range in the transmission-distribution boundary," in *IEEE Eindhoven PowerTech*, 2015, pp. 1–6.

[7] F. Capitanescu, "TSO–DSO interaction: Active distribution network power chart for TSO ancillary services provision," *Electric Power Systems Research*, vol. 163, pp. 226–230, 2018.

[8] J. Silva, J. Sumaili, R. J. Bessa, L. Seca, M. A. Matos, V. Miranda, M. Caujolle, B. Goncer, and M. Sebastian-Viana, "Estimating the active and reactive power flexibility area at the TSO-DSO interface," *IEEE Transactions on Power Systems*, vol. 33, no. 5, pp. 4741–4750, 2018.

[9] D. A. Contreras, S. Müller, and K. Rudion, "Congestion Management Using Aggregated Flexibility at the TSO-DSO Interface," in *IEEE Madrid PowerTech*, 2021, pp. 1–6.

[10] N. Majumdar, M. Sarstedt, and L. Hofmann, *Distribution grid power flexibility aggregation at multiple interconnections between the high and extra high voltage grid levels*, 2023. eprint: 2303.01107.

[11] A. Engelmann, M. B. Bandeira, and T. Faulwasser, *Approximate Dynamic Programming with Feasibility Guarantees*, 2023. arXiv: 2306.06201.

[12] C. Jones, E. C. Kerrigan, and J. Maciejowski, Eds., *Equality Set Projection: A New Algorithm for the Projection of Polytopes in Halfspace Representation*. Cambridge: Cambridge University Engineering Dept, 2004.

[13] M. Baran and F. Wu, "Network reconfiguration in distribution systems for loss reduction and load balancing," *IEEE Transactions on Power Delivery*, vol. 4, no. 2, pp. 1401–1407, 1989.

[14] N. Nazir and M. Almassalkhi, "Grid-Aware Aggregation and Realtime Disaggregation of Distributed Energy Resources in Radial Networks," *IEEE Transactions on Power Systems*, vol. 37, no. 3, pp. 1706–1717, 2022.

[15] M. Sarstedt, L. KluB, M. Dokus, L. Hofmann, and J. Gerster, "Simulation of Hierarchical Multi-Level Grid Control Strategies," in *2020 International Conference on Smart Grids and Energy Systems (SGES)*, Perth, Australia: IEEE, 2020, pp. 175–180.

[16] S. Frank and S. Rebennack, "An introduction to optimal power flow: Theory, formulation, and examples," *IIE Transactions*, vol. 48, no. 12, pp. 1172–1197, 2016.

[17] D. K. Molzahn and I. A. Hiskens, "A Survey of Relaxations and Approximations of the Power Flow Equations," *Foundations and Trends® in Electric Energy Systems*, vol. 4, no. 1-2, pp. 1–221, 2019.

[18] D. A. Contreras and K. Rudion, "Time-Based Aggregation of Flexibility at the TSO-DSO Interconnection Point," in *IEEE Power & Energy Society General Meeting (PESGM)*, 2019, pp. 1–5.

[19] S. Rakovic, E. Kerrigan, D. Mayne, and J. Lygeros, "Reachability analysis of discrete-time systems with disturbances," *IEEE Transactions on Automatic Control*, vol. 51, no. 4, pp. 546–561, 2006.

[20] A. Bemporad, M. Morari, V. Dua, and E. Pistikopoulos, "The explicit solution of model predictive control via multiparametric quadratic programming," in *IEEE American Control Conference (ACC)*, vol. 2, 2000, pp. 872–876.

[21] D. Das, D. P. Kothari, and A. Kalam, "Simple and efficient method for load flow solution of radial distribution networks," *International Journal of Electrical Power & Energy Systems*, vol. 17, no. 5, pp. 335–346, 1995.

[22] Y Latreche, "Comprehensive Review of Radial Distribution Test Systems,"

[23] M. Lubin, O. Dowson, J. Dias Garcia, J. Huchette, B. Legat, and J. P. Vielma, "JuMP 1.0: Recent improvements to a modeling language for mathematical optimization," *Mathematical Programming Computation*, 2023.

[24] A. Wächter and L. T. Biegler, "On the implementation of an interior-point filter line-search algorithm for large-scale nonlinear programming," *Mathematical programming*, vol. 106, pp. 25–57, 2006.

[25] B. Legat, "Polyhedral computation," in *JuliaCon*, 2023.

[26] K. Fukuda, "Lecture: Polyhedral Computation," Zürich, 2020.

[27] C. N. Jones, "Polyhedral Tools for Control," Ph.D. dissertation, University of Cambridge, 2005.

[28] C. N. Jones, E. C. Kerrigan, and J. M. Maciejowski, "On Polyhedral Projection and Parametric Programming," *Journal of Optimization Theory and Applications*, vol. 138, no. 2, pp. 207–220, 2008.

[29] M. Herceg, M. Kvasnica, C. N. Jones, and M. Morari, "Multi-Parametric Toolbox 3.0," in *2013 European Control Conference (ECC)*, 2013, pp. 502–510.

[30] M. Baran and F. Wu, "Optimal sizing of capacitors placed on a radial distribution system," *IEEE Transactions on Power Delivery*, vol. 4, no. 1, pp. 735–743, 1989.

[31] R. R. Jha and A. Dubey, "Coordinated Voltage Control for Conservation Voltage Reduction in Power Distribution Systems," in *IEEE Power & Energy Society General Meeting (PESGM)*, 2020, pp. 1–5.

[32] B. A. Robbins and A. D. Domínguez-García, "Optimal Reactive Power Dispatch for Voltage Regulation in Unbalanced Distribution Systems," *IEEE Transactions on Power Systems*, vol. 31, no. 4, pp. 2903–2913, 2016.

[33] P. K. Mogensen and A. N. Riseth, "Optim: A mathematical optimization package for Julia," *Journal of Open Source Software*, vol. 3, no. 24, p. 615, 2018.